

MINERALOGICAL AND GEOCHEMICAL CHARACTERIZATION OF THE ARIZLI MN DEPOSIT (AFYONKARAHISAR, TURKEY): EVIDENCE FOR DIAGENETIC AND SUPERGENE ENRICHMENT

Cihan YALÇIN^{1*} & Hatice KARA²

¹SRG Engineering and Consultancy Ltd Sti, Aydın, Türkiye; cihanyalcinjeo@gmail.com

²Department of Geological Engineering, Faculty of Engineering, Elazığ, Türkiye; haticekara@firat.edu.tr

*Corresponding author: cihanyalcinjeo@gmail.com

Abstract: The Arızlı Mn deposit (Afyonkarahisar, Türkiye) represents a diagenetic and supergene manganese mineralization system hosted within radiolarian chert-limestone alternations of an ophiolitic mélange. X-ray diffraction (XRD) analysis confirms that the primary manganese minerals are pyrolusite (MnO₂) and psilomelane [(Ba,H₂O)₂Mn₅O₁₀], with minor occurrences of quartz and calcite. Bulk geochemical analyses reveal MnO values ranging from 38.2 to 52.7 wt.%, with Mn/Fe ratios between 30 and 50, indicating enrichment in oxidized manganese. Trace element ratios, particularly Co/Zn and Ni/Co, suggest deposition under oxic conditions followed by diagenetic transformation and later-stage supergene enrichment. Discrimination diagrams – such as Fe₂O₃/TiO₂ vs. Al₂O₃/(Al₂O₃+Fe₂O₃) and Co/Zn vs. Co+Ni+Cu – indicate that the deposit shares geochemical characteristics with supergene Mn accumulations in Iran, Morocco, and North China, while contrasting with hydrothermal Mn deposits found in Turkey and Pakistan. The mineralization is structurally concentrated in faulted boundaries between ophiolitic mélange and Mesozoic carbonates, which enabled fluid migration and the remobilization of manganese. This paper introduces a comprehensive genetic model for supergene manganese deposits in ophiolitic environments, improves our comprehension of manganese metallogenesis in Tethyan ophiolitic belts, and suggests geochemical criteria relevant to the global exploration of manganese-rich sequences.

Keywords: Manganese mineralization, ophiolitic mélange, diagenetic mineralization, supergene enrichment, geochemistry

1. INTRODUCTION

Manganese (Mn) is a significant transition metal widely used in steel production, battery manufacturing, and the chemical industry, making it an indispensable global economic commodity. Manganese deposits arise from several genetic processes, including sedimentary, diagenetic, supergene, and hydrothermal origins (Öztürk, 1997; Kuleshov, 2011; Beukes et al., 2016). Comprehending these genetic processes is essential for assessing manganese ore potential and formulating successful exploration models. Turkey contains diverse kinds of manganese mineralization associated with ophiolitic mélanges, radiolarian cherts, and sedimentary environments along basin borders (Öztürk et al., 2025). The Arızlı Mn deposit (Afyonkarahisar, Türkiye) has largely remained

unexplored with respect to its mineralogical and geochemical characteristics. Understanding its formation processes is essential for grasping regional metallogenic evolution and distinguishing between primary and secondary enrichment mechanisms.

The hypothesis of supergene metallogeny has been recently reevaluated to include broader geochemical and climatic factors affecting ore genesis, providing an improved classification system for manganese and other weathering-related mineral assemblages (Wang et al., 2024). Recent breakthroughs in mineralogical research have underscored the significance of electrochemical redox mechanisms in the supergene enrichment of manganese ores, particularly in the formation of Mn-oxide minerals such as cryptomelane and psilomelane (Pinto et al., 2023). These findings

underscore the importance of using mineralogical diagnostics to assess secondary enrichment phases.

Recent studies on global manganese resources have emphasized the significance of redox-sensitive elements and the geochemistry of rare earth elements in elucidating ore-forming conditions (Xu et al., 2021). Research on manganese deposits in North China reveals that rare earth element fractionation patterns can differentiate between significant sedimentary manganese accumulations and supergene manganese enrichment (Xu et al., 2021). Paleoclimatic conditions, especially those marked by subtropical and humid weathering regimes, are essential for promoting supergene manganese enrichment, as evidenced by extensive studies from South China (Li et al., 2007a). Manganese deposits in the Aderj mining zone of Morocco exhibit a complex mineralization history, characterized by diagenetic overprinting of primary manganese sediments (Laiche et al., 2025). The formation of supergene enrichment systems may occur over extended geological timescales, involving multiple weathering and oxidation cycles. The $^{40}\text{Ar}/^{39}\text{Ar}$ date of cryptomelane in the Xinrong Mn deposit (Li et al., 2007b) has underscored the temporal intricacy of Mn ore genesis. These findings emphasize the need for mineralogical, petrographic, and geochemical data for accurate classification of Mn deposits. This study aims to determine the mineralogical composition of the Arızlı Mn deposit using X-ray diffraction (XRD) and petrographic analyses, assess major and trace element geochemistry to infer the depositional and post-depositional processes involved in Mn ore formation, and compare the geochemical signatures of the Arızlı Mn deposit with other global Mn deposits to classify it within established genetic models. This study offers new insights into the post-sedimentary alteration of manganese deposits, improving our comprehension of the genetic mechanisms that regulate manganese ore formation in Turkey. The results enhance the existing discussion on Mn metallogenesis and may guide future exploration techniques in similar geological settings.

2. GEOLOGICAL SETTING

Manganese (Mn) mineralization in Türkiye is widespread. It occurs across many geotectonic settings (Öztürk, 1997), ranging from the Triassic to the Oligocene epochs (Figure 1a). The deposits are primarily associated with the closing of the Neo-Tethyan Ocean and its subsequent tectonic history, leading to mélangé formation, radiolarian-chert deposition, and basin-margin accumulations (Göncüoğlu et al., 2015). The deposits are situated

along major suture zones, including the Paleo-Tethyan, Karakaya Complex, and the northern and southern branches of the Neo-Tethyan Ocean (Öztürk et al., 2025).

The Arızlı region is in the ophiolitic band of western Anatolia, an area shaped by the complex processes of subduction, obduction, and post-collisional extension (Dilek & Furnes, 2011; Parlak et al., 2013; Yalçın, 2025). The İzmir-Ankara-Erzincan Suture Zone (IAESZ) is a prominent tectonic barrier where the Neo-Tethyan oceanic lithosphere experienced subduction and was subsequently obducted into the Anatolide-Tauride platform (Şengör & Yılmaz, 1981). This tectonic setting has led to the formation of manganese deposits in western Anatolia, which occur within radiolarian cherts and siliceous sedimentary strata (Aydoğan, 2021).

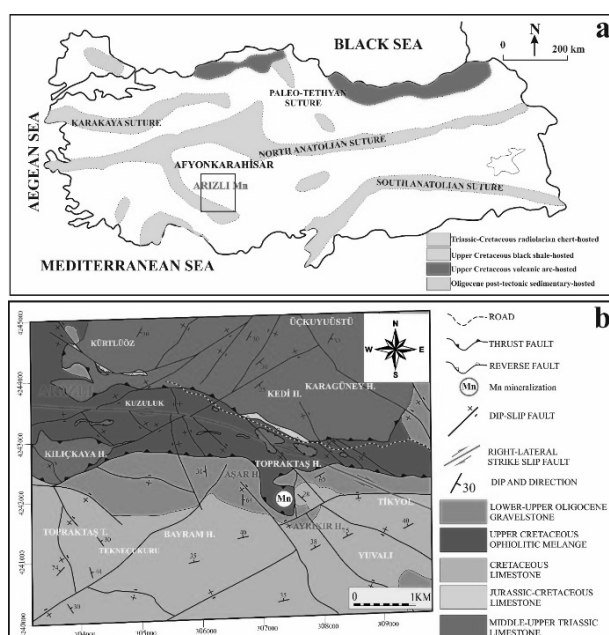


Figure 1. a. Classification and distribution of manganese deposits in Turkey according to lithological correlations and geological periods (Öztürk, 1997); b. Detailed geological map of the study area (Based on MTA L25 B4 Sheet at a scale of 1:25,000, 2023; Yalçın, 2025).

The ophiolitic sequences in the region exhibit lithological and geochemical similarities with other Tethyan-associated ophiolite belts that host manganese deposits, such as those in Iran, Pakistan, and Morocco (Laiche et al., 2025). These deposits generally develop in deep-sea settings under reducing conditions, with manganese precipitation regulated by underwater hydrothermal processes, redox-sensitive geochemistry, and post-depositional modifications (Xu et al., 2021). The geodynamic evolution of this region offers a distinctive context for assessing the origin of Mn mineralization in Türkiye (Robertson, 2002).

The Arızlı Mn deposit is in Afyonkarahisar, western Turkey. It is encompassed inside a structurally regulated ophiolitic succession (Figure 1b). The geology of the study area comprises Mesozoic to Cenozoic formations marked by tectonically complex strata affected by strike-slip faulting and folding (MTA, 2023). The primary lithological units consist of:

1. *Middle-Upper Triassic Carbonates*: These comprise the oldest formations in the region, primarily composed of limestone and dolomite. They form the pre-existing foundation upon which subsequent sedimentary and tectonic events have occurred.

2. *Jurassic-Cretaceous Limestones*: These formations overlay the Triassic carbonates and consist of thick-bedded limestone strata, indicating shallow marine depositional settings.

3. *Upper Cretaceous Ophiolitic Mélange*: This unit comprises serpentinite, dunite, harzburgite, gabbro, basalt, and radiolarian cherts. The Mn mineralization at Arızlı is located inside siliceous sedimentary layers embedded in this mélange.

4. *Oligocene Clastic Sequences*: The deposits include of flysch, conglomerates, and alluvial sediments, indicating the region's post-collisional evolution and the final stages of Neo-Tethyan closure (Yılmaz & Gürer, 2023).

The Arızlı region is characterized by a right-lateral strike-slip fault, which has proven crucial in the localization and remobilization of manganese deposits (Figure 1b). This faulting system has facilitated hydrothermal fluid circulation (Yalçın & Kaya, 2025), resulting in secondary manganese enrichment along fault zones (Afify et al., 2020).

The Arızlı Mn deposit is a structurally controlled, diagenetic-supergene manganese system where post-depositional processes, tectonic movements, and fluid interactions have modified the initial sedimentary deposits. These findings provide substantial insights into Mn metallogenesis in western Türkiye and may serve as a model for further exploration in ophiolitic environments.

3. MATERIALS AND METHODS

A total of 10 manganese ore samples were collected from various lithological units in the Arızlı region (Afyonkarahisar, Türkiye). The field survey included extensive geological mapping, focusing on lithological variations and structural features of manganese mineralization. Rock formations were systematically examined to determine stratigraphic connections and potential effects on ore deposition. Samples were carefully selected to represent the diverse mineralization styles identified in the field.

The mineralogical composition of the samples

was determined using X-ray diffraction (XRD). Analyses were conducted utilizing a BRUKER D8 ADVANCE X-ray diffractometer employing Cu K α radiation. The scanning range was set to 5°-80° (2 θ) with a step size of 0.02°. Diffraction patterns were examined utilizing the X'Pert HighScore Plus v. 3.0 software, which enabled the identification of mineral phases and a semi-quantitative evaluation of mineral abundances. XRD data provided critical insights into the crystalline structures of manganese oxides and associated gangue minerals, enhancing comprehension of alteration and post-depositional processes.

X-ray fluorescence (XRF) spectrometry was performed at the Geochemistry Research Laboratories of Istanbul Technical University. The samples were first crushed with a jaw crusher, then ground to a particle size of 45-70 μ m using a RETSCH RS-200 equipment and finally dried at 105 °C for 3 hours. Semi-quantitative XRF analyses were performed utilizing a BRUKER S8 TIGER instrument, and the accuracy of the results was corroborated with USGS DNC-1A certified reference material. The loss on ignition (LOI) was evaluated by incinerating at 1000 °C for 1.5 hours.

Before ICP-MS analysis, the samples were dissolved in a BERGHOF Speedwave™ MWS-3+ microwave disintegrator utilizing a combination of aqua regia and HF and subsequently treated with boric acid (H₃BO₃) to remove HF residues. ICP-MS analyses were performed using a PerkinElmer ELAN 6000 DRC-e instrument, with calibration standards spanning 5-100 μ g/L. Each sample solution contained 50 ppb of Re as an internal standard, and the analyses were performed in triplicate. The USGS AGV-2 and OREAS 60d were used as Certified Reference Materials (CRMs), and the study's accuracy was validated with a relative standard deviation (%RSD) of < 3 %.

4. RESULTS AND DISCUSSION

4.1. Mineralogy

The Arızlı Mn deposit is located within sedimentary layers of the ophiolitic mélange, primarily amid interbedded radiolarian chert and limestone, where Mn mineralization appears as thin, stratiform layers and impregnations over an approximate area of 100 meters (Figure 2). The mineralization is structurally controlled, taking place along the faulted boundary between the Upper Cretaceous ophiolitic mélange and Mesozoic carbonate layers (Figure 1b). The deposit exhibits a red to reddish-brown coloration, a distinguishing feature signifying oxidation and post-depositional alteration processes.

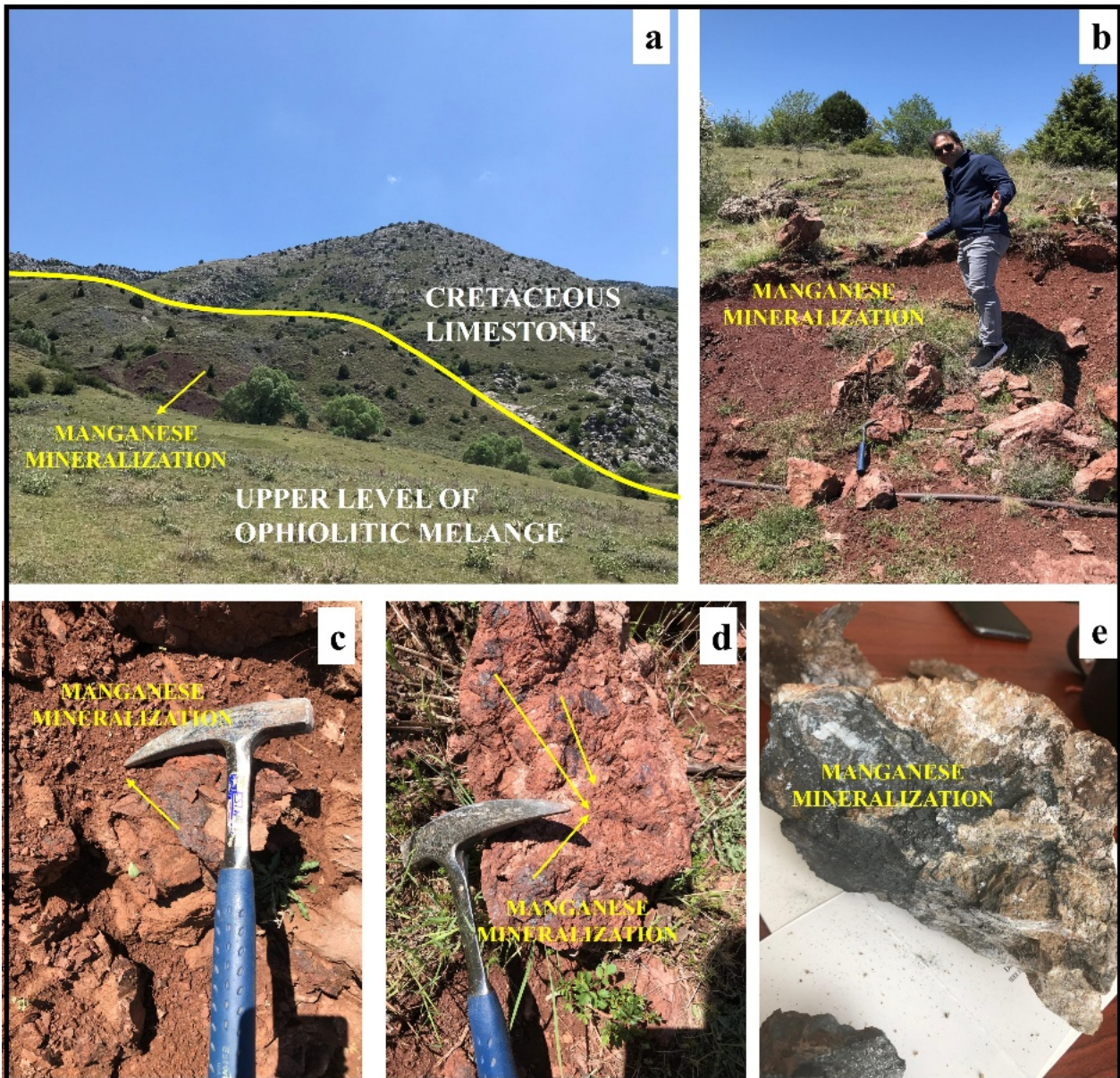


Figure 2. Overview of manganese mineralization.

An X-ray diffraction (XRD) analysis was conducted to determine the mineralogical composition of manganese-rich samples from the Arızlı deposit. The results indicate that the predominant manganese minerals are pyrolusite (MnO_2) and psilomelane ($(\text{Ba}, \text{H}_2\text{O})_2\text{Mn}_5\text{O}_{10}$), along with gangue minerals such as quartz (SiO_2) and calcite (CaCO_3) (Figure 3). Quartz and calcite are minor constituents, perhaps signifying remnants of the surrounding sedimentary matrix and diagenetic cementation. These mineral phases are located inside silicified sedimentary layers, signifying diagenetic enrichment in a deep-marine depositional environment. The identified carbonate-chert intercalations (Figure 2c-d) confirm that manganese deposits occurred during sedimentation, then mobilized by later tectonic action.

The faulty interface between the ophiolitic mélangé and Mesozoic carbonates has served as a conduit for hydrothermal fluid circulation, leading to the localized remobilization of Mn at structural discontinuities (Figure 1b). The fault-induced alteration is evident in the brecciated and iron-stained textures of manganese-rich zones (Figure 2b). The mineralization style and geochemical evidence confirm that post-depositional processes, including supergene enrichment and oxidative remobilization, have substantially modified the original Mn deposits.

4.2. Geochemistry

Geochemical analyses utilizing X-ray fluorescence (XRF) and inductively coupled plasma-mass spectrometry (ICP-MS) were performed to

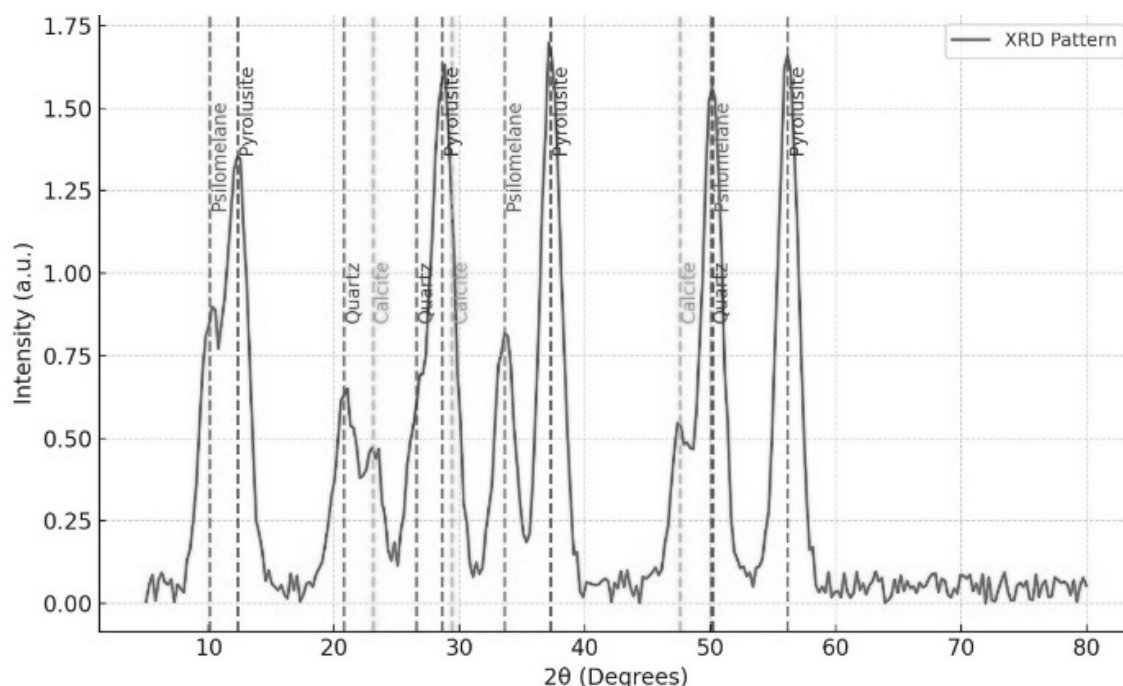


Figure 3. XRD pattern of the manganese sample.

ascertain the bulk composition of the manganese ores. The primary elemental concentrations presented in Table 1 reveal elevated MnO_2 levels (between 40 and 50 wt.%) alongside substantial Fe_2O_3 , SiO_2 , and Al_2O_3 .

The SiO_2 versus Al_2O_3 diagram (Figure 4a) and the Si versus Al diagram (Figure 4b) indicate that the Arızlı samples primarily reside within the detrital-diagenetic and pelagic sediment domains, aligning with a non-hydrothermal origin (Toth, 1980; Peters, 1988; Wonder et al., 1988). This geochemical location indicates a diagenetic origin under oxidizing and low-temperature marine conditions rather than a hydrothermal influence.

Correspondingly, the Co+Ni vs As+Cu+Mo+Pb+V+Zn discrimination diagram (Figure 4c), as per Nicholson (1992), demonstrates that the samples are situated around the region characteristic of supergene Mn-oxides. The trace element profiles, notably increased Zn and Pb levels alongside comparatively diminished Co and Ni concentrations, reinforce this conclusion. These characteristics signify oxidative weathering processes and correspond with global instances of supergene manganese enrichment (Beukes et al., 2016).

Ratios of redox-sensitive components were utilized to ascertain the depositional environment of the manganese ores. The V/Mo vs Ni/Co plot (Figure 5a) illustrates oxic conditions during manganese precipitation, with samples clustering inside the oxic region (Wright et al., 1987; Hatch & Leventhal, 1992; Gallego-Torres et al., 2010). The V/(V+Ni) versus Ni/Co plot (Figure 5b) supports an oxic depositional environment, consistent with pelagic Mn deposits

associated with the Tethyan region (Jones & Manning, 1994).

The Fe_2O_3/TiO_2 vs. $Al_2O_3/(Al_2O_3 + Fe_2O_3)$ discriminating diagram (Figure 6) was used to delineate the depositional environment better. The samples are distributed throughout the continental margin and the distal pelagic zones, corroborating the idea that manganese precipitation was influenced by both detrital input and deep-sea oxidation mechanisms (Murray, 1994). These results align with the manganese mineralization model suggested for ophiolitic-hosted deposits in Turkey (Öztürk et al., 2025) and the Vezirler Manganese Deposit (Kılıç et al., 2018). A similar relationship has been observed in the Bela ophiolite complex in Pakistan, where manganese mineralization is genetically linked to serpentinized ultramafic rocks and tectonic mélanges, suggesting analogous tectonic and lithological influences (Narejo et al., 2019).

The spider diagram (Figure 7), normalized to Upper Continental Crust (UCC) values from Rudnick & Gao (2003), indicates significant enrichments in Zn, Pb, and Sr across most samples, implying the influence of supergene processes. The low concentrations of Ni and Co may indicate limited hydrothermal input or post-depositional remobilization. Cu displays elevated values in multiple samples: however, its variability indicates a complex origin that includes both early hydrothermal inputs and later oxidative remobilization. The trace element patterns observed are analogous to supergene manganese deposits reported in Iran and Morocco (Laiche et al., 2025).

Table 1. Major Oxide and Trace Element Analyses of Samples from the Arızlı Region.

Sample (%)	AR-1	AR-2	AR-3	AR-4	AR-5	AR-6	AR-7	AR-8	AR-9	AR-10
SiO₂	4.23	5.14	3.89	2.98	4.55	5.20	3.75	3.90	3.12	2.87
Al₂O₃	2.95	4.01	3.45	3.12	4.12	2.79	3.85	3.51	4.20	3.95
Fe₂O₃	0.45	0.50	0.60	0.38	0.40	0.49	0.42	0.35	0.31	0.29
MgO	1.88	1.55	1.72	1.41	1.68	1.22	1.75	1.66	1.89	1.97
CaO	7.12	6.79	6.32	5.88	6.51	5.93	6.22	6.10	6.15	6.03
Na₂O	0.52	0.71	0.64	0.58	0.63	0.66	0.61	0.67	0.69	0.70
K₂O	0.41	0.35	0.39	0.43	0.32	0.38	0.37	0.31	0.32	0.30
TiO₂	0.029	0.032	0.035	0.030	0.027	0.034	0.028	0.026	0.025	0.024
P₂O₅	0.068	0.060	0.065	0.059	0.057	0.064	0.058	0.057	0.056	0.055
MnO	30.20	46.60	36.30	34.60	29.40	46.70	39.30	46.45	36.30	39.30
LOI	16.35	17.40	16.90	16.75	17.15	17.60	17.12	17.10	17.08	17.05
Trace Elements (ppm)										
Ni	24.60	45.20	35.70	30.80	38.90	35.04	37.13	35.51	35.48	36.41
Co	75.10	140.30	90.80	85.30	72.60	92.82	96.36	87.58	86.93	87.26
Ba	905.00	2550.00	1300.00	115.00	2000.00	1374.00	1467.80	1251.36	1241.63	1466.96
Zn	60.20	115.60	72.40	50.30	85.70	76.84	80.17	73.08	73.22	77.80
Sr	72.50	170.30	100.10	90.10	150.20	116.64	125.47	116.50	119.78	125.72
Pb	3.90	10.90	8.00	4.80	6.70	6.86	7.45	6.76	6.51	6.86
Cu	132.40	290.10	140.80	140.80	190.30	178.88	188.18	167.79	173.19	179.67
As	0.90	2.30	1.00	1.00	1.20	1.28	1.36	1.17	1.20	1.24
Mo	4.20	5.00	4.50	4.50	4.90	4.62	4.70	4.64	4.67	4.71
V	88.40	108.70	92.50	92.50	101.20	96.66	98.31	96.23	96.98	97.88
Rb	15.20	20.40	18.10	16.40	17.30	17.48	17.94	17.44	17.31	17.49
Zr	48.30	60.20	54.80	53.20	55.60	54.42	55.64	54.73	54.72	55.02
Ni/Co	1.59	1.68	1.58	1.57	1.58	1.53	1.56	1.46	1.54	1.58
Co/Zn	1.248	1.214	1.254	1.696	0.847	1.208	1.202	1.198	1.187	1.122
V/Mo	21.05	21.74	20.56	20.56	20.65	20.92	20.90	20.72	20.75	20.79
Ni %	0.35	0.42	0.38	0.33	0.41	0.46	0.50	0.41	0.54	0.49
Co %	0.22	0.25	0.24	0.21	0.26	0.30	0.32	0.28	0.35	0.31
V %	0.01	0.01	0.01	0.01	0.01	0.01	0.01	0.01	0.01	0.01
Mo %	0.0004	0.0005	0.0005	0.0005	0.0005	0.0005	0.0005	0.0005	0.0005	0.0005
Cu %	0.01	0.03	0.01	0.01	0.02	0.02	0.02	0.02	0.02	0.02
Pb %	0.0004	0.0011	0.0008	0.0005	0.0007	0.0007	0.0007	0.0007	0.0007	0.0007
Zn %	0.006	0.012	0.007	0.005	0.009	0.008	0.008	0.007	0.007	0.008
As %	0.0001	0.0002	0.0001	0.0001	0.0001	0.0001	0.0001	0.0001	0.0001	0.0001

The significant variability in trace element abundances among the Arızlı samples indicates the involvement of multiple mineralization stages, beginning with early diagenetic enrichment and subsequently followed by supergene remobilization, aligning with global instances of sediment-hosted Mn deposits (Xu et al., 2021).

In subtropical climates characterized by alternating wet and dry conditions, deep weathering profiles promote the leaching of mobile elements, leading to Mn concentration via oxidative processes (Li et al., 2007a).

Comparable weathering processes likely occurred in the Arızlı region, thereby facilitating the supergene enrichment signatures observed in the trace-element geochemistry.

The Arızlı Mn deposit illustrates distinct diagenetic and supergene enrichment processes, setting it apart from conventional sedimentary and hydrothermal manganese deposits. This study indicates a polyphase formation scenario characterized by syn-sedimentary accumulation, post-depositional diagenesis, and supergene oxidation, as evidenced by mineralogical and

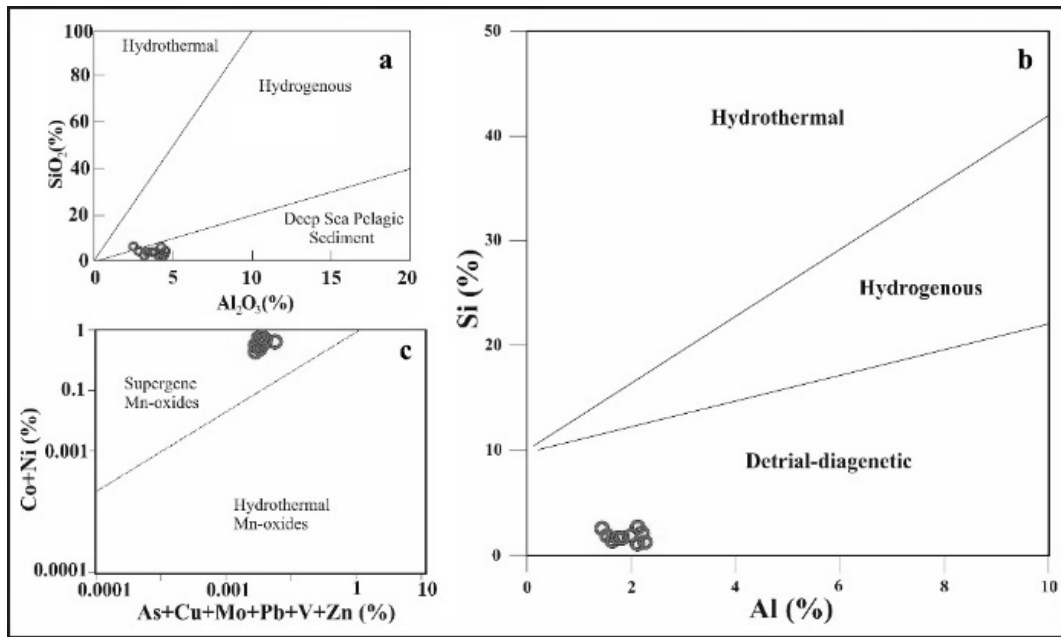


Figure 4. a. SiO_2 vs. Al_2O_3 discrimination diagram indicating the hydrothermal affinity of the studied Mn samples (Toth, 1980; Wonder et al. 1988); b. Si vs. Al discrimination diagram classifying Mn ores based on depositional environment (Peters, 1988); c. Co+Ni vs. As+Cu+Mo+Pb+V+Zn plot differentiating hydrothermal and supergene Mn-oxides (Nicholson, 1992).

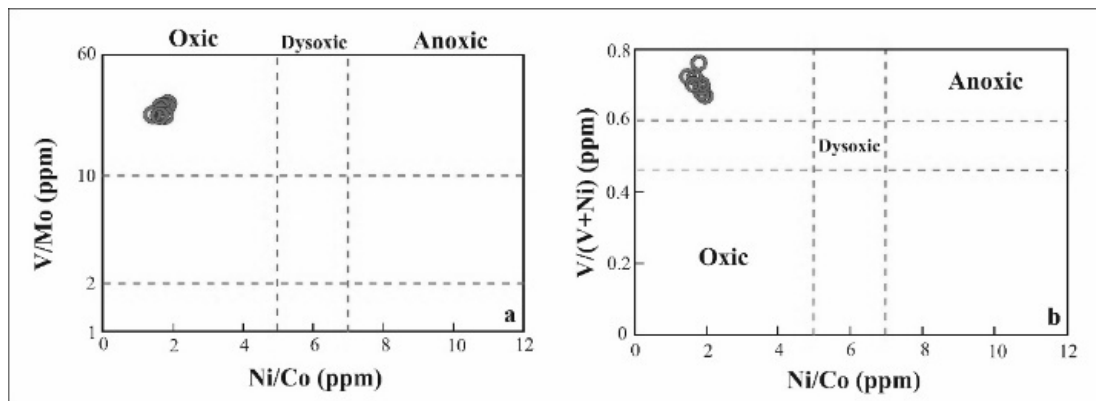


Figure 5. a. V/Mo vs. Ni/Co diagram indicating redox conditions of the depositional environment, distinguishing oxic, dysoxic, and anoxic settings (Wright et al., 1987; Öztürk et al., 2019); b. $\text{V}/(\text{V}+\text{Ni})$ vs. Ni/Co plot used to assess the redox state of manganese mineralization, confirming an oxic depositional environment.

geochemical indicators. This genetic framework aligns with global ophiolite-associated manganese deposits and provides a comparative perspective to enhance the classification of manganese mineralization. The theory proposed by Wang et al. (2024) suggests that the observed multi-phase enrichment patterns reflect a transition from syngenetic manganese accumulation to subsequent supergene enhancement, driven by prolonged fluid-rock interactions and tectonic exposure.

X-ray diffraction (XRD) and petrographic analyses indicate that manganese mineralization in Arızlı is predominantly composed of Mn-oxides, specifically pyrolusite and psilomelane, alongside minor occurrences of calcite and quartz intergrowths. Comparable Mn mineral assemblages

have been documented in the Praborna deposit (Western Alps), interpreted as resulting from hydrothermal input followed by sub-seafloor alteration (Tumiati et al., 2010). This indicates that the Arızlı Mn oxides may retain limited signatures of early protolith contributions, although the primary processes appear to be diagenetic and supergene.

The mineralogical composition, particularly the absence of Mn-carbonates such as rhodochrosite or kutnohorite (typically present in hydrothermal systems; Fan et al., 1992), indicates a non-hydrothermal origin. The presence of Fe, Ni, Co, and Zn indicate a diagenetic origin developed under reducing marine conditions, subsequently modified by oxidative weathering (Kuleshov, 2011; Laiche et al., 2025).

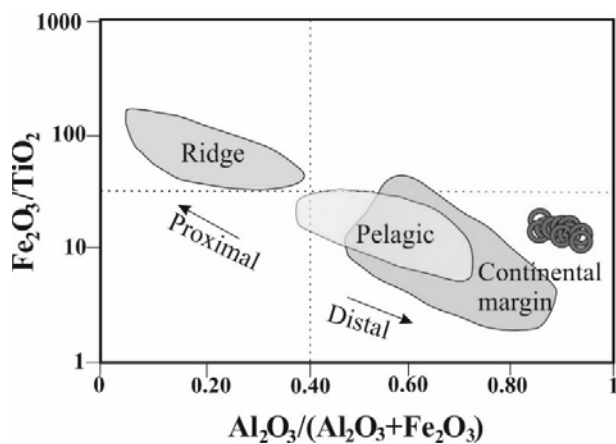


Figure 6. $\text{Fe}_2\text{O}_3/\text{TiO}_2$ vs. $\text{Al}_2\text{O}_3/(\text{Al}_2\text{O}_3+\text{Fe}_2\text{O}_3)$ discrimination diagram illustrating the depositional setting of the Arızlı Mn deposit by Murray (Murray, 1994).

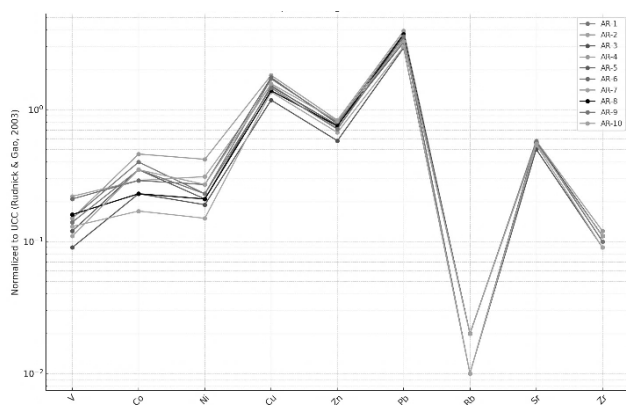


Figure 7. A multi-element spider diagram illustrates the trace-element concentrations of Arızlı Mn-ore samples (AR-1 to AR-10), normalized to Upper Continental Crust (UCC) values reported by Rudnick and Gao (2003).

Electrochemical gradients in the weathering zone facilitate the selective mobilization of Fe while maintaining Mn levels, a process documented extensively in supergene Mn-oxide deposits worldwide (Pinto et al., 2023). The residual enrichment patterns observed at Arızlı suggests a comparable process.

The moderate Mn/Fe ratio (30 - 50) at Arızlı indicates oxygenated conditions during Mn deposition, contrasting significantly with the anoxic environments of deep-sea hydrogenetic nodules and certain ophiolite-hosted Mn ores, including those in the Bela ophiolite complex (Pakistan) and Nikopol (Ukraine) (Şaşmaz et al., 2014; Narejo et al., 2019). Structural controls are critical in mineralization, with Mn-rich sediments located at tectonic contacts between ophiolitic mélangé and Mesozoic carbonates (Figure 1b). Comparable fault-controlled localization is observed in the Thrace Basin (Öztürk et al., 2025), with Mn ore bodies located along fault boundaries. The Mn units of the Karakaya Complex are regarded as hydrothermal in origin (Öztürk, 1997), yet they

exhibit similar structural settings that could have enabled redox-controlled remobilization. In Arızlı, the low Co/Zn and Ni/Co ratios – unlike hydrothermal Mn deposits in Iran and Pakistan – indicate that syn-sedimentary to early diagenetic processes, along with limited supergene enrichment, were primarily responsible for Mn concentration (Narejo et al., 2019).

While direct measurements of redox-sensitive elements like Ce are lacking, variations in trace elements (e.g., Zn, Pb, Cu, Sr) indicate that multiple mineralization stages may have impacted the Arızlı Mn ores. The enrichment of specific components and the depletion of others indicate alternating oxidative and reducing conditions that facilitated partial remobilization and reprecipitation of manganese. Paleoclimatic oscillations in western Türkiye during the Neogene and Quaternary may have promoted supergene enrichment, consistent with findings from other Mn deposits influenced by climate (Deng et al., 2017; Yılmaz & Güner, 2023). This mechanism differs from that of Mn deposits formed in arid environments, such as those in Iran and South China, where hydrothermal activity and limited water-rock interaction prevail (Li, 2000; Xu et al., 2021).

The Arızlı Mn deposit is economically significant due to its potential to augment strategic metal resources. The presence of Ni, Co, and Zn in the ore reflects the composition of essential manganese resources that serve the battery and steel industries (Beukes et al., 2016; Öztürk et al., 2019). Future exploration should focus on structurally controlled manganese mineralization zones within ophiolitic mélanges, utilizing remote sensing, drone-based geophysics, and advanced geochemical fingerprinting techniques (Dilek & Furnes, 2011).

X-ray diffraction (XRD) analysis indicates that the ore is primarily composed of Mn-oxides, specifically pyrolusite and psilomelane, along with minor amounts of quartz and calcite. Geochemical results indicate significant enrichments in Ni, Co, Zn, and Pb, suggesting a complex history of multi-phase enrichment. Discrimination diagrams utilizing Co/Zn, Ni/Co, $\text{Fe}_2\text{O}_3/\text{TiO}_2$, and $\text{Al}_2\text{O}_3/(\text{Al}_2\text{O}_3+\text{Fe}_2\text{O}_3)$ ratios indicate a genesis that is a combination of diagenetic and supergene processes, rather than being solely hydrothermal or sedimentary in origin (Kılıç et al., 2019; Narejo et al., 2019). Additionally, the possibility of hydrothermal protolith input – akin to ophiolitic metasediment-hosted manganese occurrences in the Western Alps (Tumiati et al., 2010) – should be considered in early paragenetic modeling.

The findings enhance the understanding of manganese ore formation in ophiolite-related environments, highlighting the significance of

structural architecture, redox dynamics, and paleoclimatic variability.

This study integrates mineralogical, geochemical, and structural data to establish a framework for the genetic interpretation of the Arızlı Mn deposit, offering significant implications for exploration strategies and resource evaluation.

5. CONCLUSIONS

The Arızlı manganese deposit serves as an example of a supergene and diagenetic enrichment system found within radiolarian chert-limestone alternations in an ophiolitic mélangé located in western Türkiye. Mineralogical studies reveal that pyrolusite and psilomelane are the primary manganese oxides, with minor occurrences of quartz and calcite.

The deposit displays high Mn/Fe ratios (30 - 50) and significant enrichments in trace elements, including Ni, Co, Zn, and Pb. The features suggest a complex paragenetic evolution characterized by early diagenetic manganese accumulation and subsequent supergene oxidative weathering.

Geochemical discrimination diagrams indicate a non-hydrothermal origin and exhibit similarities to sediment-hosted manganese deposits found in Morocco, North China, and Iran. Faults located at the interfaces between ophiolitic units and Mesozoic limestones significantly influenced the movement of mineralizing fluids, facilitating the mobilization and concentration of metals. The data indicate that the Arızlı deposit developed through complex interactions involving syn-sedimentary accumulation, tectonic reactivation, and near-surface oxidation processes.

This research outlines critical criteria for identifying supergene and diagenetic manganese deposits within ophiolitic environments. This underscores the diagnostic significance of trace metal geochemistry in elucidating secondary enrichment processes. Additional investigations, such as isotopic analyses and fluid inclusion studies, are advised to refine the genetic model further and evaluate the deposit's strategic metal potential.

ACKNOWLEDGEMENTS

This research includes geological investigations carried out under license number 3102414, assigned to Yılmaz Soğukçeşme. We express our gratitude to Ass. Prof. Dr. Mustafa KAYA for his support in this research.

REFERENCES

Afify, A.M., Sanz-Montero, M.E. & Osman, R.A., 2020.

Zinc-bearing ferromanganese mineralization in a rift-marginal carbonate platform, Red Sea, Egypt: Reconstruction of an epigenetic-supergenic system. *Ore Geol. Rev.*, 127, 103837.

Aydoğan, M.S., 2021. An example of ridge-proximal hydrothermal mineralisation: Evidence from radiolarian chert-hosted Fe-Mn-oxide mineralisation within the İzmir-Ankara-Erzincan Neotethyan Ocean, Central Turkey. *All Earth*, 33(1), 136-160.

Beukes, N.J., Swindell, E.P. & Wabo, H., 2016. Manganese deposits of Africa. *Episodes*, 39(2), 285-317.

Deng, Y., Ren, J., Guo, Q., Cao, J., Wang, H. & Liu, C., 2017. Rare earth geochemistry characteristics of seawater and porewater from deep sea in western Pacific. *Nat. Sci. Rep.*, 7(16539), 1-13, doi:10.1038/s41598-017-16639-1.

Dilek, Y. & Furnes, H., 2011. Ophiolite genesis and global tectonics: Geochemical and tectonic fingerprinting of ancient oceanic lithosphere. *Geol. Soc. Am. Bull.*, 123(5-6), 387-411.

Fan, D., Lui, T. & Ye, J., 1992. The process of formation of manganese carbonate deposits hosted in black shale series. *Econ. Geol.*, 87, 1419-1429.

Gallego-Torres, D., Martinez-Ruiz, F., De Lange, G.J., Jimenez-Espejo, F.J. & Ortega-Huertas, M., 2010. Trace-elemental derived paleoceanographic and paleoclimatic conditions for Pleistocene Eastern Mediterranean sapropels. *Palaeogeogr. Palaeoclimatol. Palaeoecol.*, 293, 76-89.

Göncüoğlu, M.C., Sayit, K. & Uzunçimen Keçeli, S., 2015. Evolution of the Neotethyan branches in the Eastern Mediterranean: Petrology and ages of oceanic basalts. *Turk. J. Earth Sci.*, 24(3), 249-279.

Hatch, J.R. & Leventhal, J.S., 1992. Geochemistry of manganese oxides: Redox-sensitive proxies for depositional conditions. *Chem. Geol.*, 98(1-2), 87-101.

Jones, B. & Manning, D.A.C., 1994. Comparison of geochemical indices used for the interpretation of palaeoredox conditions in ancient mudstones. *Chemical Geology*, 111, 111-129.

Kiliç, G., Selman Aydoğan, M. & Kumral, M., 2018. Preliminary results of the radiolarian-chert hosted manganese deposit within the Vezirler ophiolitic mélangé (Kula-Manisa, western Turkey): Constraints on the origin, paleo-redox conditions, and depositional environments. *Arab. J. Geosci.*, 11, 1-22.

Kuleshov, V.N., 2011. Manganese deposits: Communication I. Genetic models of manganese ore formation. *Lithol. Miner. Resour.*, 46(5), 473-493.

Laiche, M., Hinaje, S., Drissi, Y., Yaagoub, D., El Fartati, M., Ouahzizi, Y. & Laksir, A., 2025. Manganese mineralization in the northern Middle Atlas (Aderj mining zone, Morocco): petro-structural and geochemical analysis. *Heliyon*, 11, 4, e42650.

Li, J.W., Vasconcelos, P., Duzgoren-Aydin, N., Yan, D. R., Zhang, W., Deng, X.D., Zhao, X.F., Zeng, Z.P. & Hu, M.A., 2007a. Neogene weathering and supergene manganese enrichment in subtropical South China: An ⁴⁰Ar/³⁹Ar approach and paleoclimatic significance. *Earth and Planetary*

- Science Letters, 256(3–4), 389–402.
- Li, J.W., Vasconcelos, P., Zhang, W., Deng, X.D., Duzgoren-Aydin, N., Yan, D.R., Zhang, J.Q. & Hu, M.A.,** 2007b. *Timing and duration of supergene mineralization at the Xinrong manganese deposit, western Guangdong Province, South China: Cryptomelane $^{40}\text{Ar}/^{39}\text{Ar}$ dating.* Mineralium Deposita, 42, 361–383.
- Li, X.,** 2000. *Geochemistry of the Late Paleozoic radiolarian cherts within the NE Jiangxi ophiolite mélangé and its tectonic significance.* Sci. China Ser. D, v.43(6), pp.617–624, doi:10.1007/BF02879505.
- MTA,** 2023. *Geological map of Türkiye, Afyon L25 B4 Sheet, scale 1:25,000.* General Directorate of Mineral Research and Exploration (MTA), Türkiye.
- Murray, R.W.,** 1994. *Chemical criteria to identify the depositional environment of chert: general principles and applications.* Sediment. Geol., 90(3-4), 213-232.
- Narejo, A.A., Shar, A.M., Fatima, N. & Sohail, K.,** 2019. *Geochemistry and origin of Mn deposits in the Bela ophiolite complex, Balochistan, Pakistan.* Journal of Petroleum Exploration and Production Technology, 9(4), 2543–2554.
- Nicholson, K.,** 1992. *Contrasting mineralogical–geochemical signatures of manganese oxides; guides to metallogenesis.* Econ. Geol., 87(5), 1253–1264.
- Öztürk, H.,** 1997. *Manganese deposits in Turkey: distribution, types, and tectonic setting.* Ore Geol. Rev., 12, 187–203.
- Öztürk, H., Kasapçı, C. & Özbaş, F.,** 2019. *Manganese Deposits of Turkey.* In: Pirajno, F., Ünlü, T., Dönmez, C., Şahin, M. (eds) Mineral Resources of Turkey. Modern Approaches in Solid Earth Sciences, vol 16. Springer, Cham, https://doi.org/10.1007/978-3-030-02950-0_6.
- Öztürk, H., Cansu, Z., Hacilar, F. & Bolton, B.,** 2025. *Geochemistry of the Oligocene-hosted manganese ores and the host sediments in the Thrace Basin, Türkiye: Implications for genesis and exploration of the Paratethya.* Journal of Geochemical Exploration, 272, 1-16.
- Parlak, O., Çolakoğlu, A., Dönmez, C., Sayak, H., Yıldırım, N., Türkel, A. & Odabaşı, I.,** 2013. *Geochemistry and tectonic significance of ophiolites along the Izmir-Ankara-Erzincan Suture Zone in northeastern Anatolia.* Geol. Soc. Lond. Spec. Publ., 372, 5–105.
- Peters, T.,** 1988. *Geochemistry of manganese-bearing cherts associated with Alpine ophiolites.* Mar. Geol., 84(3-4), 229-238.
- Pinto, A.J., Sanchez-Pastor, N. & Jorge, R.S.,** 2023. *Electrochemical reactions driving Mn-enrichment in FeMn supergene ores: A mineralogical perspective.* Chemical Geology, 630, 121488.
- Robertson, A.H.F.,** 2002. *Overview of the Tethyan ophiolites.* Lithos, 65(1–2), 1-67.
- Rudnick, R.L. & Gao, S.,** 2003. *Composition of the continental crust.* Treatise on Geochemistry, 3, 1-64, <https://doi.org/10.1016/B0-08-043751-6/03016-4>.
- Şaşmaz, A., Türkyılmaz, B., Öztürk, N., Yavuz, F. & Kumral, M.,** 2014. *Geology and geochemistry of Middle Eocene Maden complex ferromanganese deposits from the Elazığ-Malatya region, eastern Turkey.* Ore Geol. Rev., 56, 352–372, doi:10.1016/j.oregeorev.2013.06.012.
- Şengör, A.M.C. & Yılmaz, Y.,** 1981. *Tethyan evolution of Turkey: A plate tectonic approach.* Tectonophysics, 75(3-4), 181–241.
- Toth, J.R.,** 1980. *Deposition of submarine crusts rich in manganese and iron.* Geol. Soc. Am. Bull., 91(1), 44-54, doi:10.1130/0016-7606(1980)91<44:DOSCRI>2.0.CO;2.
- Tumiati, S., Martin, S. & Godard, G.,** 2010. *Hydrothermal origin of manganese in the high-pressure ophiolite metasediments of Praborna ore deposit (Aosta Valley, Western Alps).* European Journal of Mineralogy, 22(4), 577–594.
- Wang, Q., Liu, X., Deng, J., Ramanaidou, E. & Santosh, M.,** 2024. *Supergene metallogeny: Preface.* Ore Geology Reviews, 175, 106388.
- Wonder, J.D., Spry, P.G. & Windom, K.E.,** 1988. *Geochemistry and origin of manganese-rich rocks related to iron formation and sulfide deposits, western Georgia.* Econ. Geol., 83, 1070–1081.
- Wright, J., Schrader, H. & Holser, W.,** 1987. *Paleoredox variations in ancient oceans recorded by rare earth elements in fossil apatite.* Geochim. Cosmochim. Acta, 51(3), 631–644.
- Xu, H., Gao, J., Yang, R., Feng, K., Wang, L. & Chen, J.,** 2021. *Metallogenic mechanism of large manganese deposits from Permian manganese ore belt in western South China Block: New mineralogical and geochemical evidence.* Ore Geol. Rev., 132, 103993.
- Yalçın, C. & Kaya, M.,** 2025. *Arızlı (Afyon-Şuhut) ofiyolitik melanjında krizotil oluşumlarının mineralojik, petrografik ve jeokimyasal karakterizasyonu.* Niğde Ömer Halisdemir Üniversitesi Mühendislik Bilimleri Dergisi, 14(3), 1-1.
- Yalçın, C.,** 2025. *High-resolution geophysical and geochemical assessment for Cr-Ni deposit identification in ophiolitic complexes: the Arızlı case study (Afyon, Turkey).* Baltica 38 (2), 113–129, Vilnius, ISSN 1648-858X.
- Yılmaz, Y. & Gürer, Ö.F.,** 2023. *Tectonic development of the western Anatolian extensional province.* Int. Geol. Rev., 66(3), 755–785.

Received: 14. 07. 2025
 Revised: 25. 10. 2025
 Accepted: 30. 10. 2025
 Published: 04. 11. 2025